This article has been accepted for publication in a future issue of this journal, but has not been fully edited. Content may change prior to final publication. Citation information: DOI 10.1109/LAWP.2017.2703850, IEEE Antennas and Wireless Propagation Letters

Broadband Printed-Dipole Antenna and Its Arrays for 5G Applications

Son Xuat Ta, Hosung Choo, and Ikmo Park

***Abstract*—In this paper, we propose a broadband printed-dipole antenna and its arrays for fifth-generation (5G) wireless cellular networks. To realize a wide frequency range of operation, the proposed antenna is fed by an integrated balun, which consists of a folded microstrip line and a rectangular slot. For compactness, the printed dipole is angled at 45º. The single element antenna yields a $|S_{11}| < -10$-dB bandwidth of 36.2% (26.5–38.2 GHz) and a gain of 4.5–5.8 dBi. We insert a stub between two printed-dipole antennas and obtain a low mutual coupling of < –20 dB for a 4.8-mm center-to-center spacing (0.42–0.61λ at 26–38 GHz). We demonstrate the usefulness of this antenna as a beamforming radiator by configuring 8-element linear arrays. Due to the presence of the stubs, the arrays resulted in a wider scanning angle, a higher gain, and a lower side-lobe level in the low-frequency region.**

***Index Terms*—angled dipole, beamforming, integrated balun, mutual coupling, printed antenna, 5G communication.**

I. INTRODUCTION

TO overcome the global bandwidth shortage in today's wireless cellular networks, the fifth-generation (5G) communication system is expected to utilize millimeter-wave bands [1], which have a large amount of available spectrum. Several measurements have demonstrated the promise of orders of magnitude greater bandwidths combined with further gain via beamforming and spatial multiplexing from multi-element antenna arrays [2]. As a result, designing an optimal antenna for millimeter-wave beamforming could be an important step for realizing 5G wireless cellular networks. Although there are different beamforming techniques [3], so far, the active-phased array [4], [5] is the most popular beamforming technology. Consequently, millimeter-wave phased-array antennas have recently drawn increased attention.

Manuscript received December 30, 2016. This research was supported by the Ministry of Science, ICT and Future Planning (MSIP), Korea, under the R&D program supervised by the MSIP/IITP [14-911-01-001]. This research was also supported by Civil Military Technology Cooperation (CMTC) and the Basic Science Research Program through the National Research Foundation of Korea (NRF) funded by the Ministry of Education (No. 2015R1A6A1A0303 1833).

Son Xuat Ta is with the Division of Computational Physics, Institute for Computational Science, Ton Duc Thang University, Ho Chi Minh City, Vietnam, and the Faculty of Electrical and Electronics Engineering Ton Duc Thang University, Ho Chi Minh City, Vietnam. (e-mail: tasonxuat@tdt.edu.vn).

Hosung Choo is with the School of Electronic and Electrical Engineering, Hongik University 94 Wausan-ro, Mapo-gu, Seoul 04066, Republic of Korea. (e-mail: hschoo@hongik.ac.kr)

Ikmo Park (Corresponding Author) is with the Department of Electrical and Computer Engineering, Ajou University, 206 Worldcup-ro, Youngtong-gu, Suwon 16499, Republic of Korea (e-mail: ipark@ajou.ac.kr).

In the past two decades, planar antennas have attracted interest for millimeter-wave phased arrays because of their features of wide bandwidth, low cost, ease of fabrication, and high-efficiency. Several types of planar antennas have been developed for phased array systems. Examples include quasi-Yagi antennas [6], printed dipoles [7], and angled-dipole antennas [8]–[11]. As another kind of planar antenna, T-dipole antennas fed by integrated-balun have been widely developed for wireless communications at microwave frequencies [12]–[15]. These antennas can achieve wideband or multiband operations, but their disadvantage is that they have a large size.

In this paper, we propose a broadband printed-dipole antenna for use in 5G applications. We use an integrated balun as the feed structure to enable broadband operation. The printed dipole is angled at 45º to reduce the antenna size. We demonstrate both computationally and experimentally the advantages of the single element, including compact size, broad impedance-matching bandwidth, wide radiation pattern, small gain variation, and high radiation efficiency. To achieve a low mutual coupling in the linear-array environment, we insert a microstrip stub between the two printed-dipole antennas with close spacing. The usefulness of the proposed antenna is computationally and experimentally demonstrated in beamforming radiators by configuring 8-element linear arrays. Due to the presence of stubs, the arrays result in a wider scanning angle, higher gain, and a lower side-lobe level in the low-frequency region. We use an electromagnetic simulator by CST Microwave Studio (CST MWS; Computer Simulation Technology AG., Darmstadt, Germany) for the simulations in this work.

II. SINGLE ELEMENT

Fig. 1(a) shows the geometry of the printed dipole antenna, which was designed on both sides of a Rogers RT/Duroid™ 5880 substrate ($h_s = 0.254$ mm, $\varepsilon_r = 2.2$, and $\tan\delta = 0.0009$). The antenna was composed of a 50-Ω microstrip-line feed, a truncated ground plane, an integrated balun, and a printed dipole. The feed line was on the top layer of the substrate, whereas the dipole and the ground plane were on the bottom layer. The dipole was fed by a slot line with a characteristic impedance of 116 Ω. To achieve the impedance matching over a broad frequency range, the balun acts as a microstrip-to-slot line transformer, which consists of a folded microstrip-line connected to the feedline and a rectangular slot etched on the ground plane. Impedance matching was realized by adjusting the folded line and rectangular slot. Also, the gap of the slotline (*g*) and the stripline (*gap*) are crucial design parameters of impedance matching. The printed dipole was angled to achieve a compact size, as well as to realize a wide pattern in the E-plane [16]. The antenna was characterized via CST

This article has been accepted for publication in a future issue of this journal, but has not been fully edited. Content may change prior to final publication. Citation information: DOI 10.1109/LAWP.2017.2703850, IEEE Antennas and Wireless Propagation Letters

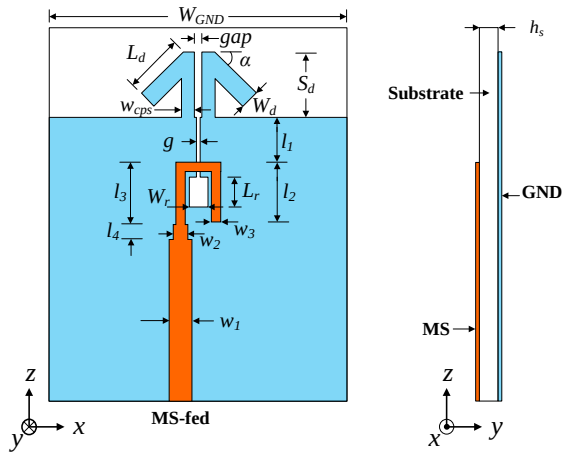

(a)

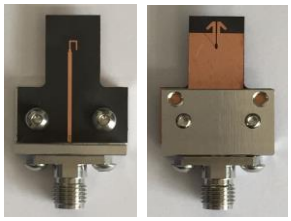

(b)

Fig. 1. (a) Geometry of the printed-dipole antenna and (b) a photograph of the fabricated sample including aluminum jig and SMA connector.

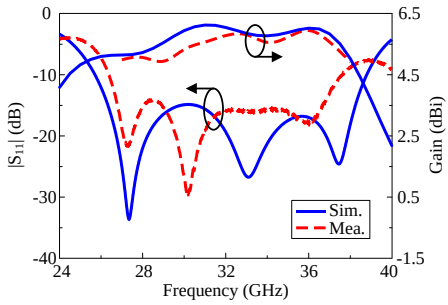

(a)

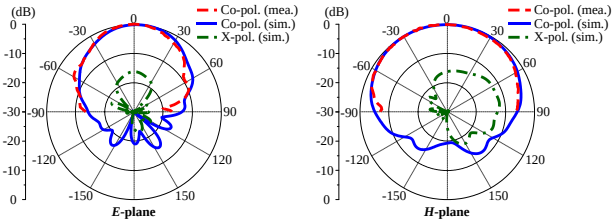

(b)

Fig. 2. The simulation and measurement results of the single element: (a) $|S_{11}|$ and gain values; (b) normalized 32-GHz radiation pattern.

Microwave Studio to ensure good impedance matching and a small gain variation at 26–38 GHz. The design parameters were: W_{GND} = 10, w_1 = 0.74, w_2 = 0.5, w_3 = 0.3, W_r = 0.4, L_r = 0.8, W_{cps} = 0.6, W_d = 0.6, L_d = 1.8, l_1 = 1.6, l_2 = 1.6, l_3 = 1.8, l_4 = 0.4, g = 0.1, gap = 0.2, S_d = 0.2, (all in millimeters) and α = 45°.

We realized the printed-dipole antenna by using printed circuit board technology. We built the antenna on both sides of a Rogers RT/Duroid™ 5880 sheet with a copper thickness of 17 μm. Fig. 1(b) shows a fabricated sample of the antenna including an aluminum jig and a 2.92 mm SMA connector (not included in the simulations). To fit the jig and SMA connector, we extended the ground plane of the fabricated antenna.

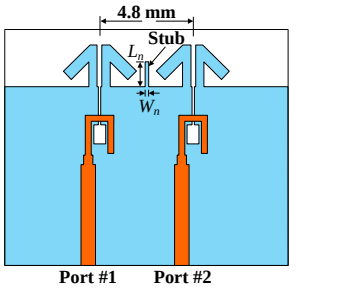

(a)

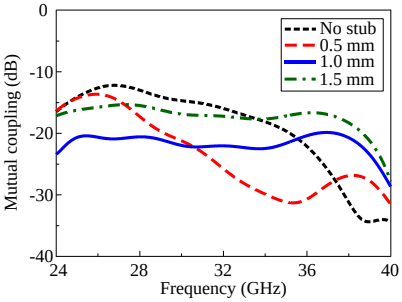

(b)

Fig. 3. (a) Geometry of the two printed-dipole antennas with a stub and a center-to-center of 4.8 mm and (b) simulated mutual coupling ($|S_{21}|$) for different lengths of the stub (L_n).

Fig. 2 presents a comparison of the measured and simulated results for the printed-dipole antenna. As shown in Fig. 2(a), the measured impedance bandwidth for $|S_{11}| < -10$ dB was 36.2% (26.5–38.2 GHz), whereas the simulated value was 40% (25.8–38.8 GHz). In addition, the antenna yielded a small gain variation. Within the operational bandwidth, the measured gain was 4.5–5.8 dBi, while the simulated value was 5.0–6.12 dBi. The slight difference between the measurement and simulation could be attributed to the effects of the jig and the SMA connector. Fig. 2(b) shows the 32-GHz radiation patterns of the antenna. The measurement results agreed with the simulations, and the two resulted in a symmetric profile in both the *E*- and *H*-planes. At 32 GHz, the antenna yielded half-power beamwidths (HPBWs) of 66° and 152° in the *E*- and *H*-planes, respectively. The patterns were also measured for other frequencies at 26.5–38.0 GHz (not shown) and are very similar to the 32-GHz patterns. Within the operational bandwidth, the measurements yielded HPBWs of 60°–70° and 150°–160° in the *E*- and *H*-planes, respectively. The measured cross-polarization was not obtained, but the simulations resulted in a value of less than –15 dB in the *E*-plane. The higher cross-polarization level in the H-plane pattern is due to the imperfect balun. The measured radiation efficiency of the antenna was not obtained, but the simulations resulted in a high value of greater than 93% at 26.0–38.0 GHz.

III. Antenna Arrays

A. Mutual Coupling

For designing antenna arrays, the tradeoff between low mutual coupling and close spacing has attracted considerable attention from researchers. To obtain a low mutual coupling for close spacing, we inserted a microstrip stub between the two printed-dipole antennas with a 4.8-mm center-to-center spacing

This article has been accepted for publication in a future issue of this journal, but has not been fully edited. Content may change prior to final publication. Citation information: DOI 10.1109/LAWP.2017.2703850, IEEE Antennas and Wireless Propagation Letters

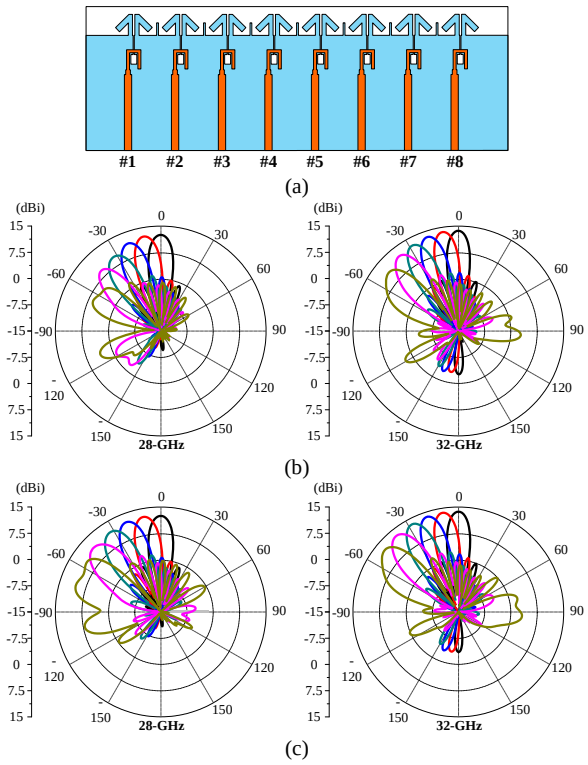

Fig. 4. (a) Geometry of an 8-element linear array with the proposed antenna, a center-to-center spacing of 4.8 mm, and stubs. Scanning performance in E-plane of the array (b) without and (c) with stubs at 28 GHz and 32 GHz.

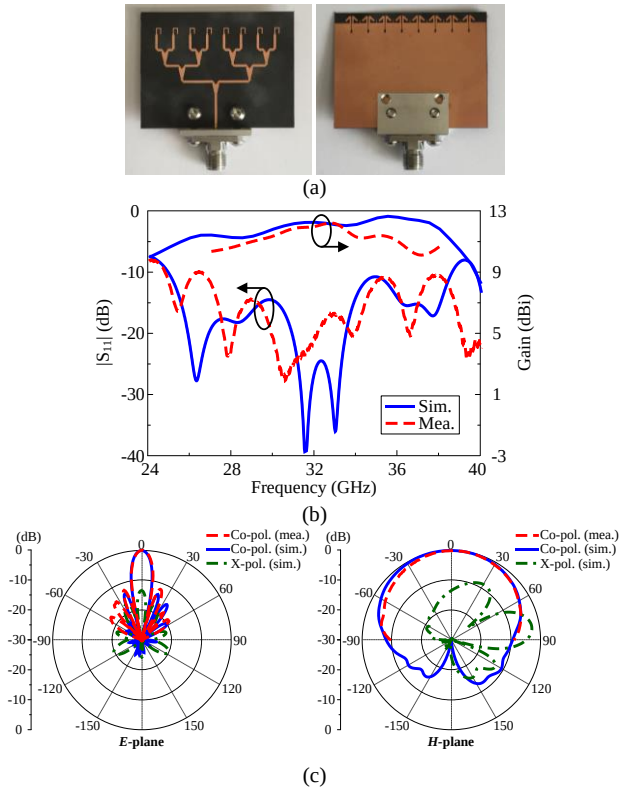

Fig. 5. (a) Fabricated sample of the 8-element array with 0º-scanning and its results: (b) $|S_{11}|$ and gain values; (c) normalized 32-GHz radiation pattern.

(0.42–0.61λ at 26–38 GHz), as shown in Fig. 3(a). The stub has a length of L_n and a width of W_n = 0.2 mm. The stub functioned in a manner similar to that of a radio frequency choke, which was designed according to the microstrip filter theory [17]. The mutual coupling characteristic is based on the LC resonance of the stub structure. The inductive and capacitive components can be controlled via adjustments to the stub length; consequently, the operating frequency can be determined by measuring L_n. This is confirmed in Fig. 3(b), which illustrates the mutual coupling between the two antennas for various values of L_n. We calculated mutual coupling as the transmission coefficient ($|S_{21}|$) from Port 1 to Port 2 of the layout. For the case without the stub (L_n = 0 mm), the mutual coupling value was greater than –15 dB in the 26–30 GHz range. $|S_{21}|$ significantly decreased in the high-frequency region (32–36 GHz) for L_n = 0.5 mm, whereas this coefficient was reduced in the low-frequency region (26–30 GHz) for L_n = 1 mm. Mutual coupling was affected in the frequency range centered at around 22 GHz for L_n = 1.5 mm (not shown). We chose L_n = 1 mm for the final design to obtain a low mutual coupling of < –20 dB across the operational bandwidth. The effects of L_n on the reflection coefficients ($|S_{11}|$ and $|S_{22}|$) were small, so they are not shown.

B. Scanning Performance

We implemented an 8-element array with the printed dipole antennas and a 4.8-mm center-to-center spacing between adjacent elements, as shown in Fig. 4(a). We calculated the scanning performance with CST Microwave Studio for the array without and with stubs, which are given in Fig. 4(b) and (c), respectively. The arrays were fed by eight ports with the same magnitude, while the scanning was achieved by the phase control at each port. Due to the lower mutual coupling between adjacent elements, the array with stubs yielded a wider scanning angle, higher gain, and a lower side lobe level (SLL) as compared to the array without the stub. At 28 GHz, the array with stubs yielded a scan angle up to 75º, a SLL of <–10 dB, and a gain of 10.4–12.5 dBi, whereas the array without stub yielded a scan angle up to 60º, a SLL of <–5 dB, and a gain of 6.2–12.5 dBi. At 32 GHz, the array with stubs yielded a scan angle up to 50º, a side-lobe level of <–13 dB, and a gain of 12.5–13.7 dBi, whereas the array without stub yielded a scan angle up to 50º, a SLL of <–9.5 dB, and a gain of 10.9–13.7 dBi. At the higher frequencies, due to the mutual coupling of <–15 dB for both configurations [Fig. 3(b)], their scanning performance is similar, so the results are not shown.

C. Eight-Element Array Measurements

To verify the scanning performance, we fabricated and measured the eight-element arrays with stubs for different fixed scanning angles. Fig. 5(a) shows a fabricated sample of the array with the 0º scanning angle. Its feeding network was a standard corporate design with T-junction power dividers and tapering transformers. Fig. 5(b) shows the simulated and measured $|S_{11}|$ and gain values of the array with 0º scanning. Both simulation and measurement resulted in a $|S_{11}| < -10$ dB at 25–38 GHz and a small gain variation; at 26.5–38 GHz, the measured gain was 10.0–12.0 dBi as compared to the simulated value of 11.5–12.5 dBi. Fig. 5(c) shows the 32 GHz radiation patterns and shows a good agreement between measurement and simulation results. The patterns of the array were also measured at 26.5–38.0 GHz (not shown) and are very similar to

This article has been accepted for publication in a future issue of this journal, but has not been fully edited. Content may change prior to final publication. Citation information: DOI 10.1109/LAWP.2017.2703850, IEEE Antennas and Wireless Propagation Letters

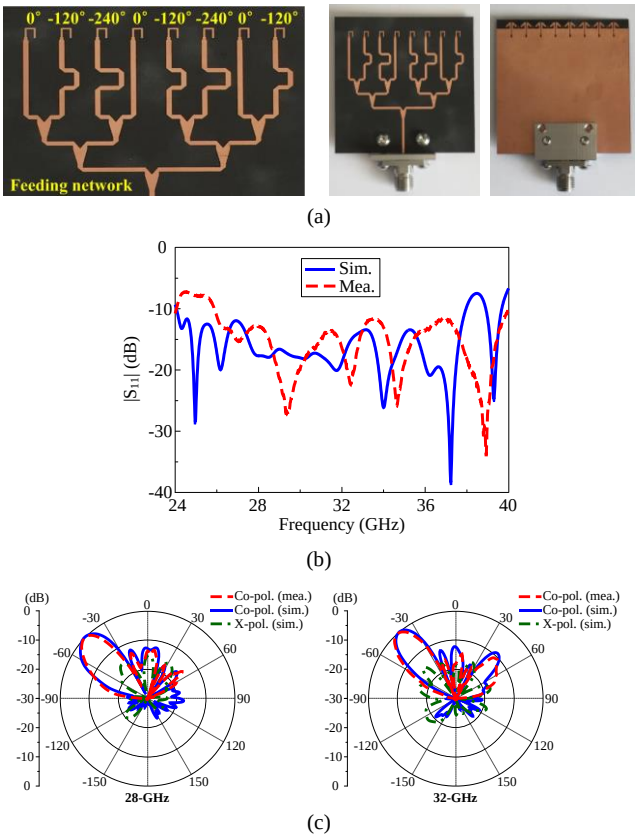

Fig. 6. (a) Fabricated sample of the 8-element array with fixed scanning angle; its (b) $|S_{11}|$ values and (c) E-plane radiation patterns at 28 GHz and 32 GHz.

the 32-GHz patterns. For the E-plane patterns, the measurements resulted in an HPBW beam width of 11.0º–13.7º and a SLL of < –12 dB. The H-plane patterns of this array were nearly identical to those of the single element with HPBWs of 150°–160°, though they yielded a higher cross-polarization level due to undesired radiation from the feeding network.

Fig. 6(a) shows a fabricated sample of the 8-element linear array with a fixed scan angle for a 4.8-mm center-to-center spacing and a microstrip stub between adjacent elements. Similar to the array with 0º scanning, we also realized the feeding network based on the T-junction power dividers and tapering transformers. As opposed to the array without scanning, this array employed fixed microstrip line delays in the feed to achieve a 45º scan angle at 28 GHz (40º scan angle at 32 GHz). The phase delays were designed for 28 GHz. Fig. 6(b) shows the simulated and measured $|S_{11}|$ of the scanning array, and shows that there is a good agreement between the two; both resulted in a $|S_{11}| < -10$ dB at 26–38 GHz. Fig. 6(c) shows the E-plane radiation patterns of the scanning array at 28 GHz and 32 GHz. At 28 GHz, the measurements resulted in an HPBW of 19º, a gain of 10.0 dBi, and a SLL of <–14 dB. At 32 GHz, the measurements resulted in a 3-dB beam width of 15º, a gain of 10.3 dBi, and a SLL of <–13 dB. These results also agreed with the values obtained by CST Microwave Studio [Fig. 4(c)]. Because of the fixed microstrip line delays, the feed network did not work well in the high-frequency region. Therefore, we did not examine the radiation patterns for the high-frequency region (above 34 GHz).

IV. Conclusions

We presented a broadband printed-dipole antenna with advantages including compact size, broad impedance-matching bandwidth, wide radiation pattern, small gain variation, and high radiation efficiency. In addition, we demonstrated the proposed antenna with applications as single-element radiators and for phased-array systems. To achieve low mutual coupling for a close center-to-center spacing, we inserted a microstrip stub between the two printed angled-dipole antennas. Moreover, due to the presence of the stubs, the array resulted in a wider scanning angle, higher gain, and a lower side-lobe level in the low-frequency region. With these advantages, the proposed antennas are good candidates for mobile terminals and base stations in 5G wireless cellular networks, as well as other millimeter-wave wireless communication systems.

References

[1] T. Rappaport, S. Sun, R. Mayzus, H. Zhao, Y. Azar, K. Wang, G. Wong, J. Schulz, M. Samimi, and F. Gutierrez, "Millimeter wave mobile communications for 5G cellular: it will work!," *IEEE Access*, vol. 1, pp. 335–349, 2013.

[2] S. Rangan, T. Rappaport, and E. Erkip, "Millimeter-wave cellular wireless networks: potentials and challenges," *Proc. IEEE*, vol. 102, no. 3, pp. 366–385, Mar. 2014.

[3] P. Hall and S. Vetterlein, "Review of radio frequency beamforming techniques for scanner and multiple beam antennas," *IEE Proceedings*, vol. 137, no. 5, pp. 293–303, Oct. 1990.

[4] D. Parker and D. Zimmermann, "Phased arrays – part I: Theory and architectures," *IEEE Trans. Microw. Theory Techn.*, vol. 50, no. 3, pp. 678–687, Mar. 2002.

[5] D. Parker and D. Zimmermann, "Phased arrays – part II: Implementations, applications, and future trends," *IEEE Trans. Microw. Theory Techn.*, vol. 50, no. 3, pp. 688–698, Mar. 2002.

[6] W. Deal, N. Kaneda, J. Sor, Y. Qian, and T. Itoh, "A new quasi-Yagi antenna for planar active antenna arrays," *IEEE Trans. Microw. Theory Tech.*, vol. 48, no. 6, pp. 910–918, Jun. 2000.

[7] Y. Suh and K. Chang, "A new millimeter-wave printed dipole phased array antenna using microstrip-fed coplanar stripline tee junction," *IEEE Trans. Antennas Propag.*, vol. 52, no. 8, pp. 2019–2026, Oct. 2008.

[8] R. Alhalabi and G. Rebeiz, "High-efficiency angled-dipole antennas for millimeter-wave phased array applications" *IEEE Trans. Antennas Propag.*, vol. 56, no. 10, pp. 3136–3142, Oct. 2008.

[9] I. Park and S. X. Ta, "Cavity-backed printed-dipole antenna for millimeter-wave applications," *Asian Workshop on Antennas and Propagation*, Busan, Korea, p. 29, Jan. 2016.

[10] S. X. Ta and I. Park, "Cavity-backed angled-dipole antennas for millimeter-wave wireless applications," *Int. J. Antennas Propag.*, vol. 2016, Article ID 5083807, 11 pages, 2016.

[11] S. X. Ta and I. Park, "Broadband printed-dipole antennas for millimeter-wave applications," *IEEE Radio and Wireless Symposium*, pp. 65–67, Phoenix, AZ, USA, Jan. 2017.

[12] B. Edward and D. Rees, "A broadband printed dipole with integrated balun," *Microw. J.*, pp. 339–344, May 1987.

[13] Q. He, B. Wang, and J. He, "Wideband and dual-band design of printed dipole antenna," *IEEE Antennas Wireless Propag. Lett.*, vol. 7, pp. 1–4, 2008.

[14] R. Li, T. Wu, B. Pan, K. Lim, J. Lascar, and M. Tentzeris, "Equivalent-circuit analysis of a broadband printed dipole with adjusted integrated balun and an array for base station applications," *IEEE Trans. Antennas Propag.*, vol. 57, no. 7, pp. 2180–2184, Jul. 2009.

[15] W. Yeoh, K. Wong, and W. Rowe, "Wideband miniaturized half bowtie printed dipole antenna with integrated balun for wireless applications," *IEEE Trans. Antennas Propag.*, vol. 59, no. 1, pp. 339–342, Jan. 2011.

[16] S. X. Ta, J. Han, H. Choo, and I. Park, "Dual-band printed dipole antenna with wide beamwidth for WLAN access points," *Microw. Opt. Tech. Lett.*, vol. 54, no. 12, pp. 2806–2811, Dec. 2012.

[17] S. Lim, W. Choi, and Y. Yoon, "Miniaturized radio frequency choke using modified stubs for high isolation in MIMO systems," *J. Electromagn. Eng. Sci.*, vol. 15, no. 4, pp. 219–223, Oct. 2015.